Binding modes of cyanide at trinuclear clusters. Crystal structure of $[Pt_3(\mu_3\text{-}CO)(CN)(dppm)_3][PF_6]$

M.C. Jennings and R.J. Puddephatt
Department of Chemistry, University of Western Ontario, London, Ont, N6A 5B7 (Canada)

Lj. Manojlović-Muir, K.W. Muir and B.N. Mwariri
Chemistry Department, University of Glasgow, Glasgow G12 8QQ, Scotland (UK)

(Received February 1, 1993; revised May 5, 1993)

Abstract

The trinuclear clusters $[M_3(\mu_3\text{-}CO)(\mu\text{-}dppm)_3]^{2+}$, dppm = $Ph_2PCH_2PPh_2$, M = Pt (**1a**), Pd (**1b**), were reacted with cyanide to give the adducts $[M_3(CN)(\mu_3\text{-}CO)(\mu\text{-}dppm)_3]^+$, M = Pt (**2a**), Pd (**2b**). Complex **2a** $[PF_6]$ has been characterized by X-ray diffraction Crystal data for **2a** $[PF_6]\cdot Me_2CO\cdot H_2O$: $P\bar{1}$, $a = 11.3731(6)$, $b = 15.4180(15)$, $c = 24.0242(29)$ Å, $\alpha = 79.839(9)$, $\beta = 82.117(7)$, $\gamma = 81.422(6)°$, $V = 4073.5(7)$ Å^3, $Z = 2$, $R = 0.047$, $R_w = 0.066$. Low temperature intermediates were characterized spectroscopically and found to be $[Pd_3(CN)_2(\mu\text{-}CO)(\mu\text{-}dppm)_3]$ and $[Pt_3(CN)(\mu\text{-}CO)(\mu\text{-}dppm)_3]^+$, with a marked difference between the Pd_3 and Pt_3 clusters. Complexes **2** were found to be fluxional in solution, with the cyanide migrating rapidly around the M_3 triangle even at low temperature. Thus, they exhibit a mobility presumably modelling that found for terminal cyanide ligands on metal surfaces. However, the binding mode of cyanide to the metal triangle appears to be different from that of CN on a Pd(111) or Pt(111) surface.

Introduction

The adsorption of CN, HCN and C_2N_2 to metal surfaces has been of much interest recently [1]. Determination of the precise binding mode of the cyanide, however, has been elusive. Since many ligands bind similarly to clusters and surfaces, a study of cyanide binding in clusters might aid in the surface assignments. Four binding modes of cyanide have been observed in transition metal complexes; modes **A–D**.

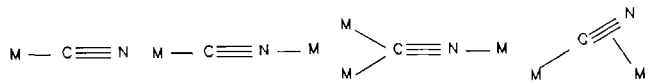

A **B** **C** **D**

There are remarkably few cyanide cluster complexes and, as far as we have been able to determine, no coordinatively unsaturated clusters to act as models for chemisorbed cyanide [2, 3]. Chemisorbed cyanide on Pd(111) and Pt(111) is believed to be bound parallel to the surface [1a, 1b], perhaps in bonding mode **D** [3], but calculations for cyanide on Ni(111) strongly suggest that cyanide should be perpendicular to the surface and bound through the carbon atom only, mode **A** [1c]. This paper reports the first cyanide adducts of coordinatively unsaturated clusters and makes comparison with isocyanides which we have previously studied. A preliminary communication of parts of this work has been published [4]. The new complexes provide a good model for the proposed perpendicular surface bonding mode of cyanide and it is shown that terminal cyanide can migrate rapidly between metal centers. Further, the low temperature intermediates have been characterized spectroscopically and shown to be different for the two trinuclear complexes studied.

Results and discussion

Complexes $[M_3(CN)(\mu_3\text{-}CO)(\mu\text{-}dppm)_3]^+$

Reaction of the clusters $[M_3(\mu_3\text{-}CO)(\mu\text{-}dppm)_3]^{2+}$, dppm = $Ph_2PCH_2PPh_2$, M = Pt (**1a**), Pd (**1b**) [5], in acetone solution at −78 °C, with one equivalent of cyanide followed by warming to room temperature gave the corresponding adducts $[M_3(CN)(\mu_3\text{-}CO)(\mu\text{-}dppm)_3]^+$, M = Pt (**2a**), Pd (**2b**), according to eqn. (1).

The reaction product **2a** was characterized crystallographically as well as spectroscopically. X-ray quality crystals of **2a** as the PF_6^- salt were grown from acetone by pentane diffusion. The structure was determined (Table 1) and an ORTEP representation is shown in Fig. 1. The three platinum atoms form a roughly equi-

0020-1693/93/$6 00

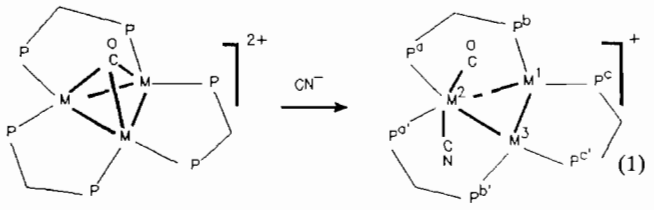

1a, M = Pt
1b, M = Pd

2a, M = Pt
2b, M = Pd

(1)

TABLE 1. Crystallographic data for $[Pt_3(CN)(\mu\text{-CO})(\mu\text{-dppm})_3][PF_6]\cdot(CH_3)_2CO\cdot H_2O$ (**2a**)

Empirical formula	$C_{80}H_{74}F_6NO_3P_7Pt_3$
Formula weight	2013 52
Space group	$P\bar{1}$
a (Å)	11.3731(6)
b (Å)	15.4180(15)
c (Å)	24 0242(29)
α (°)	79.839(9)
β (°)	82 117(7)
γ (°)	81.422(6)
V (Å^3)	4073.5(7)
Molecules in unit cell	2
D_{calc} (g cm^{-3})	1.642
Crystal dimensions (mm)	0 43×0 30×0 15
Temperature (°C)	22
Radiation	Mo Kα
Wavelength (Å)	0 71069
μ(Mo Kα) (cm^{-1})	53 8
Data collection range, θ (°)	1 5–27
Absorption factors (on F)	0.71–1.40
Unique reflections with $I>2.5\sigma(I)$	9584
Parameters refined	357
Discrepancy factor, R	0.047
R_w	0.066
Largest shift/e.s.d. ratio	0.20
Range of values in final difference synthesis (e Å^{-3})	1.5 to −1 2

lateral triangle (see Table 2 for selected bond lengths and angles) bridged by three dppm ligands. On one face of this triangle is a terminal cyanide ligand and on the other face is an asymmetrically bridging carbonyl group. The X-ray analysis could not distinguish unequivocally between the cyanide and carbonyl group, but spectroscopic data reported below prove the above assignment.

Selectively labelled derivatives **2*** (^{13}CO) and **2**** ($^{13}CN^-$) were prepared and IR analysis (see Table 3) then clearly indicated the presence of bridging carbonyl and terminal cyanide groups in both **2a** and **2b**. The structure determination, coupled with the IR analysis, revealed that the cyanide ligand in **2a** is terminally bonded to Pt(2) (Pt(2)–CN = 2.07(2) Å, Pt(2)–C–N = 177(2)°) with the Pt(2)–C–N vector nearly parallel

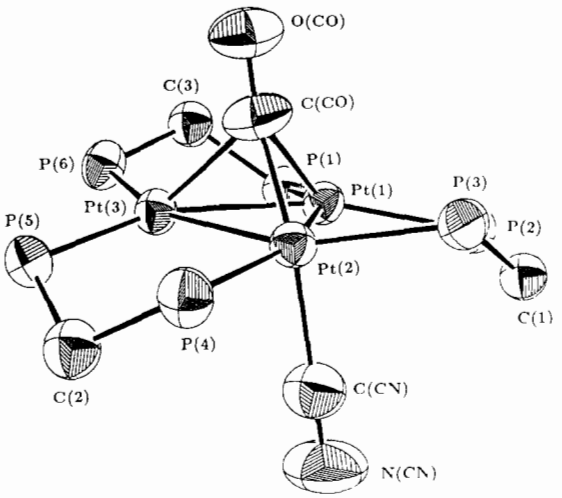

Fig 1. A view of the cation **2a** showing the coordination of the platinum atoms. 50% probability ellipsoids are displayed. Hydrogen atoms and phenyl rings are omitted for clarity.

TABLE 2. Selected interatomic distances (Å) and angles (°) in **2a**

Pt(1)–Pt(2)	2.605(1)	Pt(1)–Pt(3)	2.594(1)
Pt(1)–P(1)	2.238(4)	Pt(1)–P(2)	2 272(4)
Pt(1)–C(CO)	2.440(14)	Pt(2)–Pt(3)	2.634(1)
Pt(2)–P(3)	2.345(4)	Pt(2)–P(4)	2 347(4)
Pt(2)–C(CO)	1 935(16)	Pt(2)–C(CN)	2.071(17)
Pt(3)–P(5)	2 311(4)	Pt(3)–P(6)	2 271(4)
Pt(3)–C(CO)	2 251(17)	O(CO)–C(CO)	1 169(19)
N(CN)–C(CN)	1 144(23)	Pt(3) .C(CN)	3.557(16)
Pt(1) ..C(CN)	3 270(16)		
Pt(2)–Pt(1)–Pt(3)	60.9(1)	Pt(2)–Pt(1)–P(1)	153 3(1)
Pt(2)–Pt(1)–P(2)	96.7(1)	Pt(2)–Pt(1)–C(CO)	45.0(4)
Pt(3)–Pt(1)–P(1)	93.3(1)	Pt(3)–Pt(1)–P(2)	156.3(1)
Pt(3)–Pt(1)–C(CO)	53.0(4)	P(1)–Pt(1)–P(2)	107.6(2)
P(1)–Pt(1)–C(CO)	125 7(4)	P(2)–Pt(1)–C(CO)	117.6(4)
Pt(1)–Pt(2)–Pt(3)	59.4(1)	Pt(1)–Pt(2)–P(3)	92.3(1)
Pt(1)–Pt(2)–P(4)	154.0(1)	Pt(1)–Pt(2)–C(CO)	63 0(5)
Pt(1)–Pt(2)–C(CN)	88 0(5)	Pt(3)–Pt(2)–P(3)	149 7(1)
Pt(3)–Pt(2)–P(4)	95.1(1)	Pt(3)–Pt(2)–C(CO)	56.6(5)
Pt(3)–Pt(2)–C(CN)	97.5(5)	P(3)–Pt(2)–P(4)	113.7(2)
P(3)–Pt(2)–C(CO)	102 8(5)	P(3)–Pt(2)–C(CN)	91.5(5)
P(4)–Pt(2)–C(CO)	109.1(5)	P(4)–Pt(2)–C(CN)	90.6(5)
C(CO)–Pt(2)–C(CN)	147 7(7)	Pt(1)–Pt(3)–Pt(2)	59.8(1)
Pt(1)–Pt(3)–P(5)	153.6(1)	Pt(1)–Pt(3)–P(6)	96 3(1)
Pt(1)–Pt(3)–C(CO)	60 0(4)	Pt(2)–Pt(3)–P(5)	95.2(1)
Pt(2)–Pt(3)–P(6)	155.4(1)	Pt(2)–Pt(3)–C(CO)	45.8(4)
P(5)–Pt(3)–P(6)	109.3(2)	P(5)–Pt(3)–C(CO)	110.1(4)
P(6)–Pt(3)–C(CO)	119.5(5)	Pt(1)–C(CO)–Pt(2)	72.0(5)
Pt(1)–C(CO)–Pt(3)	67.0(4)	Pt(1)–C(CO)–O(CO)	125.8(11)
Pt(2)–C(CO)–Pt(3)	77 6(6)	Pt(2)–C(CO)–O(CO)	156.9(13)
Pt(3)–C(CO)–O(CO)	121.2(13)	Pt(2)–C(CN)–N(CN)	176.7(15)

with the normal to the Pt_3 plane (intervector angle 10.1°). The Pt(1)–C(CN) and Pt(3)–C(CN) distances are clearly non-bonding (Table 2). The carbonyl ligand bridges the Pt_3 triangle in a very asymmetric fashion:

the Pt(2)–C(CO) distance of 1.94(2) Å is very much shorter than the Pt(1)–C(CO) and Pt(3)–C(CO) distances of 2.44(2) and 2.25(2) Å. This geometry for the carbonyl is similar to that found in $[Pt_3(\mu_3\text{-}CO)\{P(OPh)_3\}(\mu\text{-dppm})_3]^{2+}$, with Pt–C distances of 1.93(3), 2.16(3) and 2.27(3) Å, and is also consistent with the trend observed in related triplatinum cluster complexes [6].

The IR assignments for clusters **2** were not immediately obvious. For example, **2a** contained IR bands at 2114 and 1807 cm^{-1} (Nujol mulls), but it is not clear which band is due to the carbonyl and which to the cyanide ligand. Selective isotopic labelling (Table 3) showed clearly that $\nu(CO) = 1807$ and $\nu(CN) = 2114$ cm^{-1} and hence that carbonyl is bridging and cyanide terminal. Solution IR data confirmed that the cyanide in **2a** remained terminal in solution in CH_2Cl_2. For both **2a** and **2b** the experimental ratios of frequencies $\nu(^{12}CO)/\nu(^{13}CO)$ or $\nu(^{12}CN)/\nu(^{13}CN)$ agreed well with the theoretical values.

The solid state structure for **2** has only two-fold symmetry and the ^{31}P NMR spectrum is therefore expected to contain three resonances due to dppm phosphorus atoms [6]. However, only a single resonance was observed for **2a** or **2b** at temperatures down to −90 °C, indicating that the cluster cations are fluxional. The ^{13}C NMR spectra, at room temperature or −80 °C, of **2a*** (Fig. 2) contained a 1:4:7:4:1 quintet due to coupling to ^{195}Pt, indicating the presence of an apparently triply bridging carbonyl ($\delta(CO) = 197$ ppm, $^2J(PC) = 10$, $^1J(PtC) = 636$ Hz). A similar intensity pattern is seen in the cyanide region of the ^{13}C NMR spectrum of **2a**** (Fig. 3), although it is less clear since resonances due to the phenyl ring carbons appear in the same spectral region. The cyanide ($\delta(CN) = 126.8$ ppm) signal couples to all three of the ^{195}Pt atoms with a coupling of 427 Hz, suggesting a triply bridging cyanide. The spectrum of **2a***** (^{13}CO, ^{13}CN labelled) showed the additional coupling $^2J(^{13}C^{13}C) = 32$ Hz between the carbon atoms on either face of the Pt_3 triangle (Figs. 2 and 3, lower curves). Since the X-ray structure and IR data together show that the cyanide is actually terminal, these NMR data establish that **2a** is fluxional, with the cyanide ligand migrating rapidly around the Pt_3 triangle as shown in eqn. (2). Further, the observation of the couplings $^1J(Pt\text{–}CO)$, $^1J(Pt\text{–}CN)$ and $^2J(CO\text{–}CN)$ in the fast fluxionality regime shows that the process occurs without dissociation of either the carbonyl or cyanide ligand from the cluster. It is not possible to distinguish between transition states having μ_2-CN or μ_3-CN groups for the cyanide migration, but eqn. (2) shows the simpler mechanism with a μ_3-CN intermediate.

TABLE 3. Cyanide and carbonyl IR data for complexes **2**

Complex[a]	Code	ν(CO)	$\nu(^{13}CO)$	ν(CN)	$\nu(^{13}CN)$
$[Pt_3(\mu_3\text{-}CO)]^{2+}$	**1a**	1765			
$[Pt_3(\mu_3\text{-}CO)(CN)]^+$	**2a**	1807		2114	
$[Pt_3(\mu_3\text{-}^{13}CO)(CN)]^+$	**2a***		1769	2114	
$[Pt_3(\mu_3\text{-}CO)(^{13}CN)]^+$	**2a****	1807			2066
$[Pd_3(\mu_3\text{-}CO)]^{2+}$	**1b**	1860			
$[Pd_3(\mu_3\text{-}CO)(CN)]^+$	**2b**	1823		2133	
$[Pd_3(\mu_3\text{-}^{13}CO)(CN)]^+$	**2b***		1784	2133	
$[Pd_3(\mu_3\text{-}CO)(^{13}CN)]^+$	**2b****	1823			2095

[a]These formulae omit the dppm and the PF_6 anion.

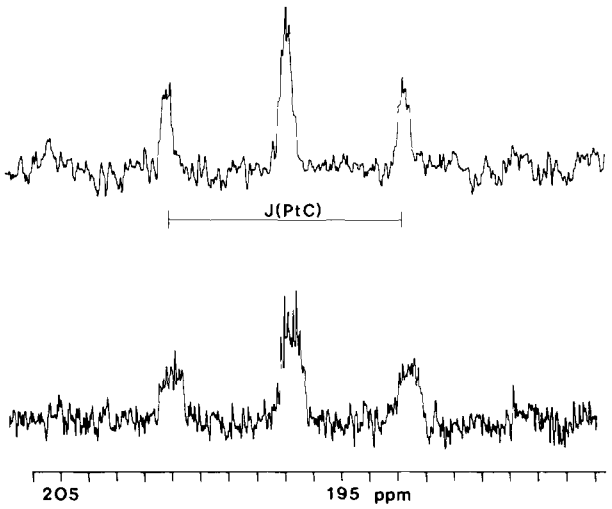

Fig. 2. Carbonyl region of ^{13}C NMR spectra (75.43 MHz) of $[Pt_3(\mu_3\text{-}*CO)(CN)(dppm)_3][PF_6]$ (**2a***) (upper curve) and $[Pt_3(\mu_3\text{-}*CO)(*CN)(dppm)_3][PF_6]$ (**2a*****) (lower curve); the extra doublet splitting is due to $^2J(^{13}CO\text{–}^{13}CN)$.

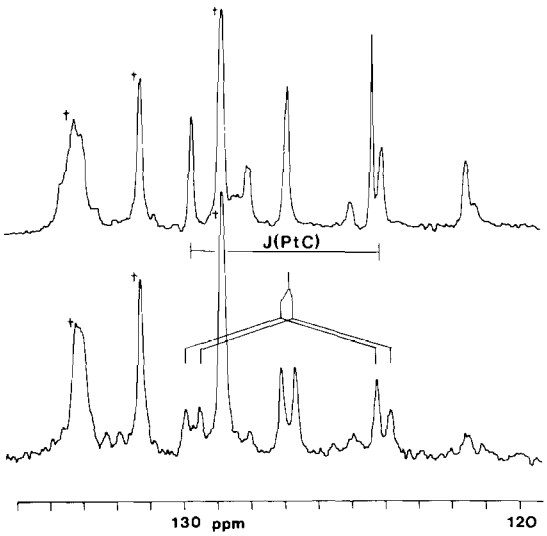

Fig. 3. Cyanide region of ^{13}C NMR spectra (75.43 MHz) of $[Pt_3(\mu_3\text{-}CO)(*CN)(dppm)_3][PF_6]$ (**2a****) (upper curve) and $[Pt_3(\mu_3\text{-}*CO)(*CN)(dppm)_3][PF_6]$ (**2a*****) (lower curve); the extra doublet splitting is due to $^2J(^{13}CO\text{–}^{13}CN)$. Marked peaks are due to phenyl carbons.

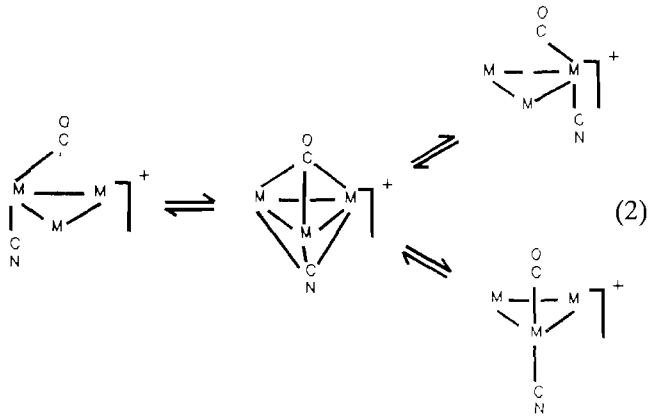

(2)

Reaction intermediates

While the complexes **2** have the same structure for M = Pd and Pt, intermediates in their formation from **1** and CN^- at low temperature were different. Low temperature multinuclear NMR studies were carried out and the intermediates were characterized as $[Pt_3(CN)(\mu_2\text{-}CO)(\mu\text{-}dppm)_3]^+$ (**3**) and $[Pd_3(CN)_2(\mu_2\text{-}CO)(\mu\text{-}dppm)_3]$ (**4**).

Species **3** is stable at −40 °C and yields three distinct signals in the ^{31}P NMR spectrum (Fig. 4) implying that the molecule possesses a plane of symmetry. The structure of **3** is proposed to be similar to that for a low temperature intermediate formed in the reaction of **1a** with methyl isocyanide and characterized as $[Pt_3(\mu\text{-}CO)(CNMe)(\mu\text{-}dppm)_3]^{2+}$ [6]. Table 4 compares the ^{31}P NMR data for $[Pt_3(\mu\text{-}CO)(CN)(\mu\text{-}dppm)_3]^+$ (**3**) and $[Pt_3(\mu\text{-}CO)(CNMe)(\mu\text{-}dppm)_3]^{2+}$ showing the similarities. Complex **3** was not fluxional at −40 °C and gave a ^{13}C resonance for the cyanide ligand at $\delta = 132$

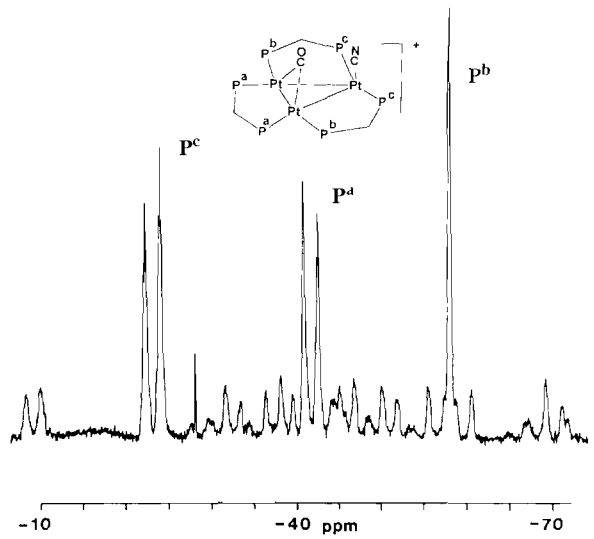

Fig. 4. ^{31}P NMR spectrum (121.4 MHz) of $[Pt_3(\mu_2\text{-}CO)(CN)(dppm)_3][PF_6]$ (**3**) at −40 °C.

TABLE 4 ^{31}P NMR data for comparison between **3** and $[Pt_3(\mu\text{-}CO)(CNMe)(\mu\text{-}dppm)_3]^{2+}$

	$\delta(^{31}P)$ (ppm)	$^3J(PP)$	$^1J(PtP)$	$^2J(PtP)$
$[Pt_3(\mu\text{-}CO)(CN)]^+$ (**3**)	−25 9	212	3380	
	−43.7	212	2240	
	−61.1	228[a]	2920	412
$[Pt_3(\mu\text{-}CO)(CNMe)]^{2+}$	−20 6	197	3512	
	−43.0	195	2080	254
	−51 2	174[a]	3232	337

[a]This coupling is between two chemically equivalent phosphorus atoms.

which appeared as a 1:4:1 triplet due to $^1J(PtC) = 984$ Hz, as expected for a terminal cyanide [2b, 2c]. In addition, the ^{13}C NMR spectrum revealed the presence of a doubly bridging carbonyl ligand (verified by platinum satellite intensities) at $\delta = 232$, with two sets of platinum satellites. A coupling of 20 Hz is observed between these two carbon atoms.

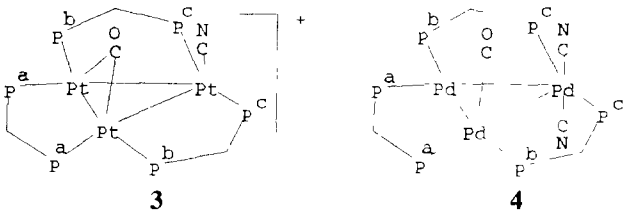

3 **4**

Since the NMR spectra of **2a** are essentially the same from room temperature to −80 °C, it is clear that **3** is not just a low temperature form of **2a** although it has the same formula. Thus we infer that the cyanide and carbonyl ligands in **3** are on the same face of the platinum triangle. This is the structure which would be formed by kinetic control if cyanide adds to the side of the platinum triangle which is less sterically hindered by the phenyl substituents of the μ-dppm ligands. Isomerization of **3** to **2a** would require dissociation of either the cyanide or, less likely, the carbonyl ligand followed by recoordination on the opposite face of the Pt_3 triangle [6].

Complex **2a** reacted with excess iodomethane to give the iodide complex $[Pt_3(\mu_3\text{-}CO)(\mu_3\text{-}I)(\mu\text{-}dppm)_3][PF_6]$ with displacement of cyanide, presumably as MeNC.

Multinuclear, variable temperature, NMR experiments were carried out to characterize the intermediate palladium cluster **4**. The synthesis of **4**, even at −78 °C, was always accompanied by some formation of the final product **2b** but the spectra of **4** were clearly resolved. This species possessed three distinct phosphorus signals (Fig. 5) indicating that the molecule has only two-fold symmetry. The experiments were repeated with both ^{13}CO enriched **1b** and ^{13}C enriched sodium cyanide. The ^{13}C NMR spectrum revealed a carbonyl

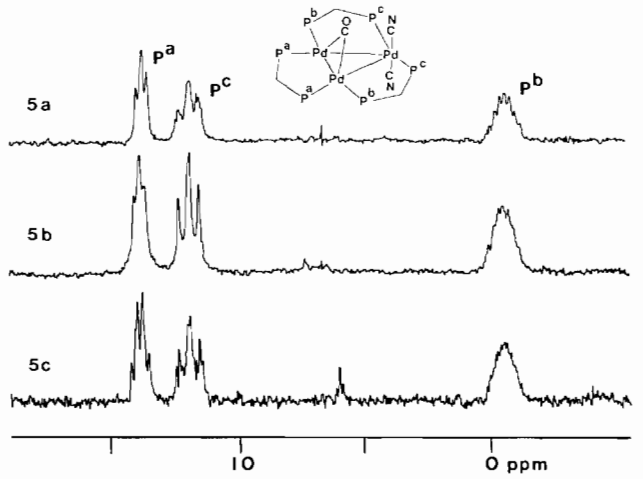

Fig. 5. ^{31}P NMR spectra (121.4 MHz) at -40 °C of **4**. (a) $[Pd_3(\mu_2\text{-}CO)(*CN)_2(dppm)_3]$, the coupling $^2J(P^c\text{–}^{13}CN)$ is partially resolved (compare with spectrum (b); (b) $[Pd_3(\mu_2\text{-}CO)(CN)_2(dppm)_3]$; (c) $[Pd_3(\mu_2\text{-}*CO)(*CN)_2(dppm)_3]$, note the doublet splitting due to $^2J(P^a\text{–}^{13}CO)$.

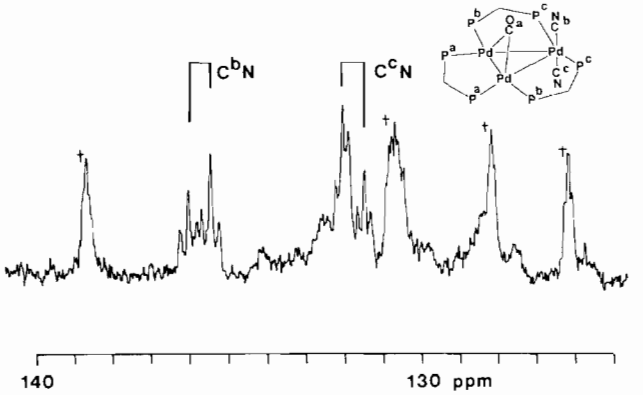

Fig 6. ^{13}C NMR spectrum (75.43 MHz) of $[Pd_3(\mu_2\text{-}*CO)(*CN)_2(dppm)_3]$ at -80 °C. The 'AB' splitting due to $^2J(^{13}CN\text{–}^{13}CN)$ is indicated above (marked peaks are due to phenyl carbons)

signal at $\delta = 235.3$ which is in the chemical shift region of bridging carbonyls. For example, the μ_2-CO signal for the platinum cluster **3** appears at $\delta = 232.3$. In addition, two cyanide signals were observed at $\delta = 135.5$ and 131.7, with coupling $^2J(CC) = 42$ Hz, leading to an AB spectral pattern (Fig. 6), but there was no measurable coupling between the cyanide and carbonyl carbons. The two cyanide signals also have triplet splittings due to $^2J(PC)$ coupling. On this basis, the cluster **4** is deduced to contain a doubly bridging carbonyl ligand on one face of the palladium triangle and two terminal cyanide ligands bound to the same palladium atom but on opposite faces of the triangle. It is easy to see that loss of one of the cyanide ligands from **4** would give the final product **2b**. However, it is less obvious why the low temperature intermediate should contain two cyanide ligands.

Reaction of the palladium cluster **1b** with excess cyanide ions can be controlled to a limited extent. If the cluster **1b** is reacted with three molar equivalents of potassium cyanide at low temperature (-78 °C) then an orange powder is isolated. This complex, **5**, is characterized as $[Pd_2(CN)_2(\mu\text{-dppm})_2]$. It gives a ^{31}P NMR signal at $\delta = -6.9$ and a ^{13}CN signal at $\delta = 141$, with $J(PC) = 11.6$ Hz. The mass spectrum of **5** contained a molecular ion peak, confirming the formula $[Pd_2(CN)_2(\mu\text{-dppm})_2]$. The conversion of **1b** to **5** occurs in high yield.

Conclusions

Both the palladium and platinum clusters **1** react with one equivalent of cyanide to give the analogous products **2**, albeit in slightly better yield for the platinum cluster. Both products **2** possess a rapidly migrating cyanide ligand and a triply bridging carbonyl group. The difference arises in the low temperature intermediates. The intermediate **3** contains a bridging carbonyl and a terminal cyanide on the same side of the triplatinum triangle. The palladium cluster, however, reacts rapidly by addition of two cyanides to give **4**. Cluster **4** is structurally similar to **3**, but with a second cyanide added *trans* to the first. In all cases, the cyanide binds as a terminal ligand, whereas the carbonyl ligand is either triply or doubly bridging.

The above data clearly establish that, in these model complexes, cyanide has a lower tendency than the isoelectronic carbonyl to act as a μ_2-C- or μ_3-C bonded ligand (or a higher tendency to act as a terminal ligand) on the Pd_3 or Pt_3 triangle. No evidence for the bonding mode **D**, thought to be present on the Pd(111) or Pt(111) surface [1], was found; this bonding mode, in which cyanide acts as a 4-electron ligand, is theoretically possible since the clusters **2** are still coordinatively unsaturated (44e clusters). Instead, the terminal cyanide bonding can be considered to model cyanide adsorbed on Ni(111) and several other metal surfaces [1]. The very easy mobility of terminal cyanide between metal centers, established here for the first time, suggests that a similar surface mobility can be expected and indicates that there is only a small energy difference between terminal and bridging cyanide bonding modes.

Experimental

NMR spectra were recorded with Varian XL-200 (^1H) and XL-300 ($^{13}C\{^1H\}$, $^{31}P\{^1H\}$ and $^{195}Pt\{^1H\}$) spectrometers, using acetone-d^6 as solvent unless otherwise specified. Chemical shifts are quoted with respect to Me_4Si (^1H, ^{13}C), H_3PO_4 (^{31}P) and aqueous K_2PtCl_4

(^{195}Pt). IR spectra were recorded by using a Bruker IR/32 FTIR spectrometer, and FAB mass spectra were recorded on a Finnigan MAT 8230 mass spectrometer, with samples prepared as mulls in oxalic acid/3-mercapto-1,2-propanediol. Elemental analyses were carried out by Guelph Chemical Laboratories. Complexes **1a** and **1b** were prepared as described elsewhere [7]. KCN was purchased from Aldrich and Na^{13}CN was purchased from MSD Isotopes.

[Pt$_3$(μ_3-CO)(CN)(μ-dppm)$_3$][PF$_6$] (2a)

To a suspension of **1a** (72.3 mg, 35.2 μmol) in methanol (10 ml), cooled to −78 °C, was added slowly a methanolic KCN solution (7.5 ml of 4.87×10^{-3} M solution, 36.6 μmol). The orange suspension changed to give a dark brown solution. The reaction mixture was stirred for 1 h at −78 °C and then 1 h at room temperature, resulting in a clear orange solution. Monitoring by ^{31}P NMR spectroscopy revealed formation of a single product in almost quantitative yield. The product was isolated as an orange solid and purified by dissolving in acetone (2–3 ml), filtering to remove some pale yellow insoluble powder, and precipitation by pentane. M.p. = 260 °C. *Anal.* Calc. for [Pt$_3$(μ_3-CO)(CN)(dppm)$_3$][PF$_6$]·2 acetone: C, 45.95; H, 3.63; N, 0.65. Found: C, 45.33; H, 3.80; N, 0.8%. MS: *m/z* = 1791 {Pt$_3$(CO)(CN)(dppm)$_3^+$ = 1791}, 1764 {Pt$_3$(CO)(dppm)$_3^+$ = 1763}. NMR data: ^{1}H, δ = 7.4–6.9 [m, 60H], 5.6 [br s, ^3J(PtH) = 42. Hz, CH_2P_2]; ^{31}P, δ = −20.9 [s, ^1J(PtP) = 3223, ^2J(PtP) = 84, ^3J(PP′) = 182 Hz, dppm]; ^{195}Pt (CD_2Cl_2), δ = −2632 [br t, ^1J(PtP) = 3200 Hz]; ^{13}C (CD_2Cl_2), δ = 197 [dm, $^2J(C^aC^b)$ = 32.3, $^2J(C^aP)$ = 9.6, $^1J(C^aPt)$ = 636 Hz, C^aO], 126.8 [d, $^2J(C^aC^b)$ = 32.3, $^1J(C^bPt)$ = 427 Hz, C^bN].

Typical NMR tube experiment of reaction of 1a with KCN

The platinum cluster **1a** (58.7 mg, 28.5 μmol) was dissolved in CD_2Cl_2 (0.8 ml) and transferred to a septum sealed 5 mm NMR tube. This was cooled to −78 °C in a dry ice bath. A molar equivalent of KCN or Na^{13}CN in methanol solution (160 μl of 0.184 M, 29.4 μmol) was added to the NMR tube at low temperature and the tube was quickly inserted into the NMR probe at −80 °C. ^{31}P and ^{13}C NMR spectra were recorded at −40 °C and ambient temperature. The final reaction solution was evaporated to dryness, the residue was dissolved in acetone, the solution was filtered, and the product was precipitated with pentane and dried *in vacuo*. This gave a clean final product which was then examined using IR spectroscopy. These experiments were repeated using both the ^{13}C enriched carbonyl of **1a** and ^{13}C labelled sodium cyanide to allow full characterization of the low temperature intermediates. NMR data: **3**: −40 °C, ^{31}P (CD_2Cl_2), δ −25.9 [m, $^3J(P^aP^c)$ = 212, $^2J(P^cP)$ = 13, $^1J(PtP^c)$ = 3380 Hz, P^c], −43.7 [m, $^3J(P^aP^c)$ = 212, $^2J(P^bP^a)$ = 13, $^1J(PtP^a)$ = 2240 Hz, P^a], −61.1 [t, $^2J(P^bP^a)$ = 13, $^1J(PtP^b)$ = 2920, $^2J(PtP^b)$ = 412, $^3J(P^bP^{b'})$ = 228 Hz, P^b]; ^{13}C (CD_2Cl_2), δ = 232.3 [d, $^2J(C^aC^b)$ = 20, $^1J(PtC^a)$ = 860, $^2J(PtC^a)$ = 130 Hz, μ-C^aO], 131.7 [d, $^2J(C^aC^b)$ = 20, $^1J(PtC^b)$ = 984 Hz, C^bN].

[Pd$_3$(μ_3-CO)(CN)(dppm)$_3$][PF$_6$] (2b)

This was prepared similarly from **1b** (63.1 mg, 35.2 μmol) in methanol (7 ml) with methanolic KCN (200 μl of 0.183 M solution, 36.6 μmol) at −78 °C. The reaction mixture was stirred for 25 min at −78 °C, then allowed to warm to room temperature giving a brown–purple solution. The product was isolated as a dark brown solid. Yield 90%. M.p. 168–174 °C. NMR data: **2b**: ^{31}P (CD_2Cl_2), δ −13.7 [s, dppm], ^{13}C (CD_2Cl), δ 200.1 [quin, $^2J(C^aP)$ = 9.2 Hz, coupling observed at −40 °C, μ_3-C^aO], 140.4 [t, $^2J(C^bP)$ = 12 Hz, C^bN].

Typical NMR tube experiment of reaction of 1b with KCN

The palladium cluster **1b** (28 mg, 15.6 μmol) was dissolved in CD_2Cl_2 (0.8 ml) in a septum sealed 5 mm NMR tube. This was cooled to −78 °C and 0.09 ml of a methanolic potassium cyanide solution (0.182 M, 16.4 μmol) was added. ^{31}P and ^{13}C NMR spectra were recorded at −40 °C and then at ambient temperature. Spectroscopic yield of the final product **2b** was observed to be 80–90%. The product was dried *in vacuo* to afford a dark powder and was examined using IR spectroscopy. These experiments were repeated using both the ^{13}C enriched carbonyl of **1b** and ^{13}C labelled sodium cyanide to allow full characterization of the low temperature intermediates. NMR data: **4** at −40 °C, ^{31}P (CD_2Cl_2), δ 13.8 [t, $^2J(P^aP^b)$ = 26, $^2J(P^aC^a)$ = 29 Hz, P^a], 11.8 [t, $^2J(P^bP^c)$ = 50 Hz, P^c], −0.6 [tt, $^2J(P^bP^c)$ = 50, $^2J(P^aP^b)$ = 26 Hz, P^b]; ^{13}C (CD_2Cl_2), δ 235.3 [m, $^2J(P^aC^a)$ = 29, μ-C^aO], 135.5 [td, $^2J(CP)$ = 17, $^2J(C^bC^c)$ = 42 Hz, C^bN], 131.7 [td, $^2J(CP)$ = 12, $^2J(C^bC^c)$ = 42 Hz, C^cN].

X-ray structure determination of 2a[PF$_6$]·Me$_2$CO·H$_2$O

All X-ray measurements were made at 22 °C with graphite-monochromated Mo Kα radiation and an Enraf-Nonius CAD4 diffractometer. Two red, plate-like crystals of [Pt$_3$(CO)(CN)(μ-dppm)$_3$][PF$_6$]·$(CH_3)_2CO$·H_2O were used. The first was mounted in air and showed a rapid decline in the intensity of the scattering, presumably because of solvent loss. The second crystal was therefore enclosed in a Lindemann glass capillary. It showed the forms {100}, {010} and {001}. Experimental details are summarized in Table 1.

The unit cell constants were determined by the least-squares treatment of 23 reflections with Bragg angles in the range $13 < \theta < 15°$. The crystals were found to

be triclinic on the basis of their observed metric and Laue symmetry. The assumption that the space group was $P\bar{1}$ led to a successful structure analysis.

Intensities for 18 720 reflections with h: 0 to 14, k: −19 to 19, l: −24 to 24 were measured by continuous $\omega/2\theta$ scans. The scan speeds were adjusted to give $\sigma(I)/I < 0.03$, subject to a time limit of 80 s for low angle data ($1.5 < \theta < 21°$) and 120 s for high angle data ($\theta > 21°$). Two reflections, (2 0 0) and (0 0 2), were used to monitor the stability of the crystal and the diffractometer. Their intensities showed random variations of ±6% and ±2.1% over the period of the data collection. Lorentz and polarization factors were applied to the intensities. Empirical absorption corrections were made by the method of Walker and Stuart [8] at the end of the isotropic refinement. The internal agreement factor, R_{int}, for merging 1834 duplicate intensities was 0.123 before and 0.066 after correction for absorption. Of 17 739 unique reflections measured, 9584 for which $I > 2.5\sigma(I)$ were used in the subsequent analysis.

The positions of the non-hydrogen atoms were obtained using Patterson and difference Fourier methods. Hydrogen atoms of the dppm ligands were included in calculated positions with U (isotropic) fixed at 0.070 Å^2. The structure was refined by minimizing the function $\Sigma w(|F_o| - |F_c|)^2$ where $w = \sigma(|F_o|)^{-2}$. The phenyl rings were constrained to D_{6h} symmetry with C–C = 1.38 Å. Isotropic displacement parameters were refined for phenyl, methylene, acetone and water non-H atoms; for other non-H atoms U_{ij} were refined (see 'Supplementary material').

The parameters of non-H atoms defining acetone and water molecules of solvation were included in the refinement. The highest peaks (1.0–1.5 e/Å^3) in the final difference synthesis suggested that the asymmetric unit might contain a second, partially occupied acetone site; attempts to model the electron density at this site were not successful.

An alternative to the model described involves bridging CN and terminal CO ligands. Refinement of such a model gave essentially identical agreement indices to those in Table 1 but somewhat less plausible vibrational ellipsoids than those in Fig. 1. Figure 1 thus represents the more reasonable interpretation of the X-ray data; however, these by themselves do not completely exclude the alternative model with bridging CN and terminal CO.

The GX program package [9] was used for all calculations; atomic scattering factors and anomalous dispersion corrections were taken from the International Tables for X-ray Crystallography [10].

Supplementary material

Tables of fractional coordinates, hydrogen atom parameters, anisotropic displacement parameters, bond lengths, angles and observed and calculated structure factors are available from the authors on request.

Acknowledgements

We thank NSERC (Canada), NATO, SERC (UK) for financial support and the Kenyan High Commission for a studentship (to B.N.M).

References

1 (a) M.E Kordesch, W. Stenzel and H Conrad, *Surf Sci, 186* (1987) 601; (b) P.L. Hagans, X. Guo, I. Chorkendorff, A Winkler, H Siddiqui and J T. Yates, Jr., *Surf Sci, 203* (1988) 1; (c) X.-Y. Zhou, D.-H Shi and P.-L. Cao, *Surf. Sci, 223* (1989) 393; (d) J.S. Somers, M.E Kordesch, R. Hemmen, Th. Lindner, H. Conrad and A M. Bradshaw, *Surf Sci, 198* (1988) 400; (e) J.M. Lindquist, J.P. Ziegler and J.C. Hemminger, *Surf. Sci, 210* (1989) 27.

2 (a) A.G. Sharpe, *The Chemistry of Cyano Complexes of the Transition Metals,* Academic Press, London, 1976; (b) T.G. Appleton, J.R. Hall and M.R. Williams, *Aust. J Chem, 40* (1987) 1565; (c) C. Brown, B R. Heaton and J. Sabounchei, *J. Organomet. Chem., 142* (1977) 413; (d) L.E Manzer and G.W. Parshall, *Inorg Chem, 15* (1976) 3114.

3 (a) M.D. Curtis, K.R. Han and W.M. Butler, *Inorg Chem., 19* (1980) 2096; (b) H.C. Aspinall, A.J Deeming and S. Donovan-Mtunzi, *J Chem Soc., Dalton Trans,* (1983) 2669, (c) S.P. Deraniyagala and K.R. Grundy, *Inorg Chim Acta, 84* (1984) 205.

4 M.C. Jennings, R J. Puddephatt, Lj Manljlović-Muir, K.W. Muir and B N. Mwariri, *Organometallics, 11* (1992) 4164.

5 R.J. Puddephatt, Lj. Manojlvić-Muir and K.W. Muir, *Polyhedron, 9* (1990) 2767, and refs. therein

6 (a) A.M Bradford, G. Douglas, Lj. Manojlović-Muir, K.W. Muir and R.J. Puddephatt, *Organometallics, 9* (1990) 409; (b) R.J. Puddephatt, M. Rashidi and J.J. Vittal, *J Chem. Soc., Dalton Trans,* (1991) 2835

7 (a) G. Ferguson, B.R. Lloyd and R.J. Puddephatt, *Organometallics, 5* (1986) 344; (b) Lj. Manojlović-Muir, K.W. Muir, B.R. Lloyd and R.J. Puddephatt, *J Chem. Soc, Chem Commun,* (1983) 1336.

8 N. Walker and D. Stuart, *Acta Crystallogr, Sect A, 39* (1983) 158.

9 P.R. Mallinson and K.W. Muir, *J. Appl Crystallogr., 18* (1985) 51.

10 *International Tables for X-ray Crystallography,* Vol. IV, Kynoch, Birmingham, UK, 1974.